Indonesian Journal of Electrical Engineering and Computer Science
Vol. 24, No. 1, October 2021, pp. 167~177
ISSN: 2502-4752, DOI: 10.11591/ijeecs.v24.i1.pp167-177

High precision brain tumor classification model based on deep transfer learning and stacking concepts

Halima El Hamdaoui[1], Anass Benfares[2], Saïd Boujraf[3], Nour El Houda Chaoui[4], Badreddine Alami[5], Mustapha Maaroufi[6], Hassan Qjidaa[7]
[1,4]Laboratory of Artificial Intelligence, Data Sciences and Emerging Systems,
Sidi Mohamed Ben Abdellah University of Fez, Fez, Morocco
[2,7]Department of Physics, Faculty of Science, Sidi Mohamed Ben Abdellah University of Fez, Fez, Morocco
[3]Department of Biophysics and Clinical MRI Methods, Faculty of Medicine,
Sidi Mohamed Ben Abdellah University of Fez, Fez, Morocco
[5,6]Department of Radiology and Clinical Imaging, University Hospital of Fez, Fez, Morocco

Article Info

Article history:

Received May 7, 2021
Revised Aug 17, 2021
Accepted Aug 23, 2021

Keywords:

Brain tumors classification
Convolutional neural networks
Deep transfer learning
High grade glioma
Low grad glioma
Stacking model

ABSTRACT

In this article, we proposed an intelligent clinical decision support system for the detection and classification of brain tumor from risk of malignancy index (RMI) images. To overcome the lack of labeled training data needed to train convolutional neural networks, we have used a deep transfer learning and stacking concepts. For this, we choosed seven convolutional neural networks (CNN) architectures already pre-trained on an ImageNet dataset that we precisely fit on magnetic resonance imaging (MRI) of brain tumors collected from the brain tumor segmentation (BraTS) 19 database. To improve the accuracy of our global model, we only predict as output the prediction that obtained the maximum score among the predictions of the seven pre-trained CNNs. We used a 10-way cross-validation approach to assess the performance of our main 2-class model: low-grade glioma (LGG) and high-grade glioma (HGG) brain tumors. A comparison of the results of our proposed model with those published in the literature, shows that our proposed model is more efficient than those published with an average test precision of 98.67%, an average f1 score of 98.62%, a test precision average of 98.06% and an average test sensitivity of 98.33%.

Corresponding Author:

Hassan Qjidaa
Department of Physics, Faculty of Science
Sidi Mohamed Ben Abdellah University of Fez
Fez, Morroco
Email: hassan.qjidaa@usmba.ac.ma

1. INTRODUCTION

Today, specialists use often the magnetic resonance imaging (MRI) to diagnose clinically brain [1]. Thus brain diseases have become detectable with great precision thanks to the high resolution, the strong contrast and the segmentation of the tissues [2]. In addition, a precise classification allowing a good discrimination of diseased tissues and normal tissues of the MRI image has become essential for planning a good surgery, detecting and predicting brain disease [3]. Currently, researchers have succeeded in detecting the contours of different brain tissues with good precision, thus making it possible to accurately and automatically measure the volume of lesions in the brain [4].

The abnormal multiplication of brain cells is a definition of brain tumor [5], [6]. The latter can be benign or malignant. The brain tumor causes severe damage thus endangering the patient's life. According to

statistics published in [7] more than 18,000 people will die of brain tumors in 2020. Less dangerous cancers are meningioma and glioma. On the other hand, two families of its cancers, namely astrocytoma and glioblastoma, are more aggressive [8] with a greater degree of malinity for glioblastoma [9] causing the successive death of cells in the affected region [10].

Among the tools for the general detection of different classes of tumor is MRI where each class of tumor manifests itself with a different contrast on the MRI image [11], [12]. The MRI will help the doctor to make a good diagnosis of the tumor in order to offer an adequate treatment which will depend on the location, size, shape, type and grade of the cancer. However, these characteristics will vary from one patient to another, thus requiring good classification and strong recognition of the cancer to ensure adequate treatment [13]. In addition, the doctor's intervention in the visual detection of the tumor and the manual monitoring of its evolution are often accompanied by errors [14] or the need to set up an automated system for the recognition and classification of its tumors.

Extracting the shape and texture of the regions of interest from the MRI image are essential steps in classifying brain tumor of the brain [15]. The computer-assisted diagnostic (CAD) system constitutes a tool, well known in the literature, for diagnosing these tumors [16]. Two essential components form the backbone of any CAD system; i) component relates to the stages of pretreatment and detection of the tumor and ii) component relates to the classification of the tumor.

In this paper, we will rely on our work developed by our team concerning the application of deep learning in the health field [17] to propose a new method of classifying brain tumors from MRI. To achieve this goal, we propose a model based on transfer learning to reduce the learning stages and speed up the entire training process. The transfer model offers a promising alternative to refine an already pre-trained convolutional neural networks (CNN) on a large dataset like ImageNet. Furthermore, we will use brain MRI images from the BraTS database [18] to train our proposed classification model.

In literature, deep learning theme has been dealt with by a few researchers [19]. Among the limitations mentioned by these related works we find the scarcity and low number of MR images labeled by specialists who are essential for training neural networks. To overcome the lack of labeled training data needed to train convolutional neural networks, we present, in this article, a high precision brain tumors automatic classification system based on deep transfer learning and stacking concepts. Indeed, the use of the deep transfer learning concept eliminates the cost of complex layer parameters and the long validation processes and the use of stacking model improve the classification accuracy. The stacking process will promote the prediction of true positives by selecting the prediction that obtained the best prediction score. This will automatically increase accuracy and sensitivity. We use a 10-way cross-validation approach to assess the performance of our main 2-class model; low-grade glioma (LGG) and high-grade glioma (HGG) brain tumors. Indeed, this choice allowed us to earn two points for accuracy compared to the choice of 5-fold cross-validation. A comparison of the results of our proposed model with those published in the literature, shows that our proposed model is more efficient than those published with an average test precision of 98.67%, an average f1 score of 98.62%, a test precision average of 98.06% and an average test sensitivity of 98.33%.

The remainder of the paper discussed as follows; section 1 discussed the importance of detecting brain tumor and background review. In section 2, we present the methodology of developing our classification model based on deep transfer laearning and staking models. In section 3, we present our simulation results. We end our article with a discussion followed by a general conclusion.

2. MATERIALS AND METHODS

We used an HP Intel Core I9-10900F computer clocked at 10x2.80Ghz (10x5.20Ghz Turbo)-Nvidia 8GB GPU - 32GB DDR4 2933Mhz RAM to develop our CNN architectures through the Keras library under Python. We used cross entropy to estimate the loss function, Adam to optimize the training parameters of the different models and 60 iterations as the maximum training time.

2.1. Dataset

In this work, MR images of brain tumors are collected from BraTS 2019 data [20]. An update of this database, mainly composed of high degree glioblastoma (HGG) and low degree glioma (LGG), was recently carried out by adding 3T MRI images annotated by specialists. Examples LGG and HGG tumor MR images extracted from the BraTS 2019 database acquired under the four modalities; native volumes (T1), weighted in T1 after type of contrast (T1Gd), type T2 (T2) and T2 fluid inversion type recovery (FLAIR) are shown in Figures 1(a)-(h). The resolution of its RM images is 240x240x155. Furthermore, BraTS 2019 dataset contains 210 images of cases HGG and 75 images of cases LGG. We have converted the images of this dataset from 3D to 2D, we obtained 26532 images 2D of case LGG and 94284 images 2D of case HGG so

we selected 26532 images from HGG to balance these two classes. In the experimental analysis, 85% of the data set was used as training and validating and 15% was used as the test set. A summary of the distribution of the data used in our simulations are given by Table 1.

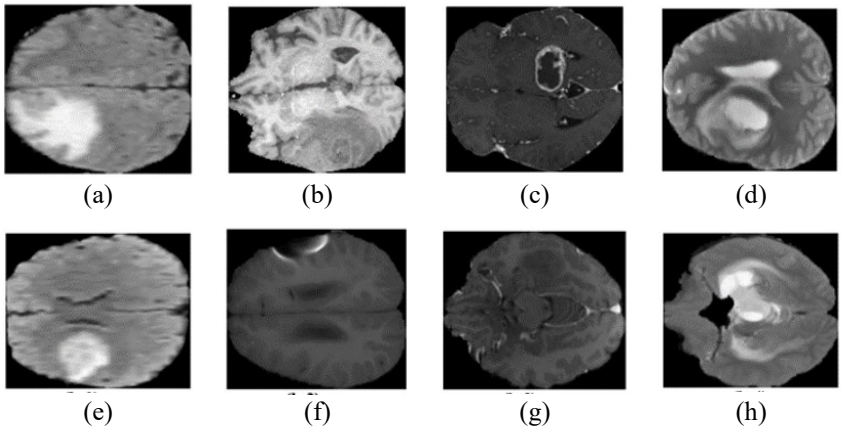

Figure 1. Brain tumor MRI images of the two classes with multi-modality: (a) HGG-Flair, (b) HGG-T1, (c) HGG-T1ce, (d) HGG-T2, (e) LGG-Flair, (f) LGG-T1, (g) LGG-T1ce, and (h) LGG-T2

Table 1. Dataset summary

Disease	Number of images	Training data	Testing data
HGG	26532	22565	3967
LGG	26532	22539	3993

2.2. Data pre-processing and augmentation

Most of the collected risk of malignancy index (RMI) images have a larger or smaller black area surrounding the image of the brain. This unwanted outer area can be a problem during the learning process. Indeed, our models can take this area as a defining characteristic to discriminate LGG from HGG tumors. Therefore, to solve this issue, we create a script that removes these unwanted outer area from the samples, an example of this process is illustrated in Figures 2(a) and 2(b). After solving the black bars issue, we will deal with the lack of sufficient amount of training data by using an Image Data Augmentation for Deep Transfer Learning to better generalize our model and avoid over-fitting. We used, horizontal flipping and scaling.

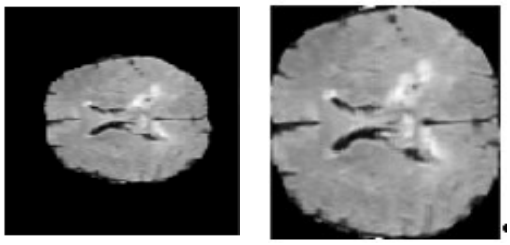

Figure 2. Removing of unwanted outer area from the image: (a) original image and (b) cropped image

2.3. Proposed deep transfer learning and stacking CNN model

Often, forming a CNN from scratch is generally difficult as this process required large training data as well as significant expertise to select appropriate model architecture for appropriate convergence. To overcome this problem, we propose a model that combines two notions; deep transfer learning and the stacking model. Indeed, deep learning transfer eliminates the expense of the many parameters of hidden layers and the immense validation processsus of our proposed model. The stacking model can automatically combine the best votes of several models by selecting as output prediction having had a maximum number of votes. For this we will use seven CNN architectures already pre-trained on an ImageNet dataset that we will precisely fit on a dataset of brain tumor images collected from the BraTS 2019 database.

2.4. Proposed deep transfer learning model

The deep transfer learning offers a promising alternative to refine an already pre-trained CNN on a large dataset like ImageNet using its weights. This helps us to speed up the convergence process during training. At this step, the process uses seven, as is shown in Figure 3, already pre-trained CNN extracted from the ImageNet database; InceptionResNetV2 [21], DenseNet121 [22], MobileNet [23], InceptionV3 [24], Xception [25], and VGG16 and VGG19 [26]. The classification and prediction process is carried out through a fully connected CNN network made up of multiple classifiers.

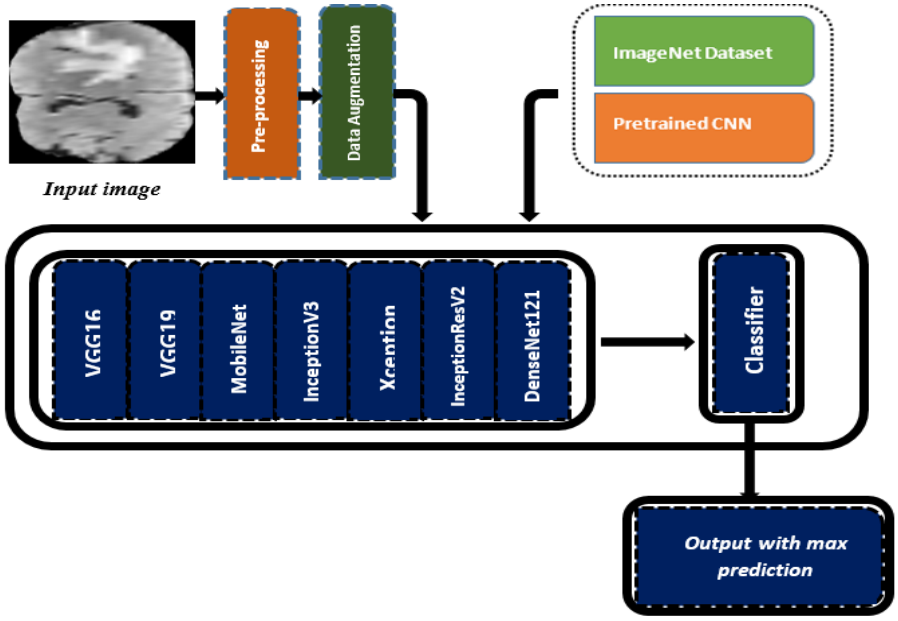

Figure 3. Proposed deep transfer learning process

2.5. Stacking model

In the remaining section we present our new Stacking model that we developed. The latter is based on the neural network sub-models integrated into an overall stacking model. Our model allowed us to find the best way to combine the predictions of several existing models already pre-trained. Consequently, we will develop a stacking model using 7 neural networks as a sub-model and a scikit-learn classifier as a meta-learner. The basic idea of this approach is to consider the prediction of each network by assigning it a score. Once the seven networks have finished their prediction, the score obtained by each prediction is counted. Only the prediction with the highest score is selected as output from the model, as is shown in Figure 4.

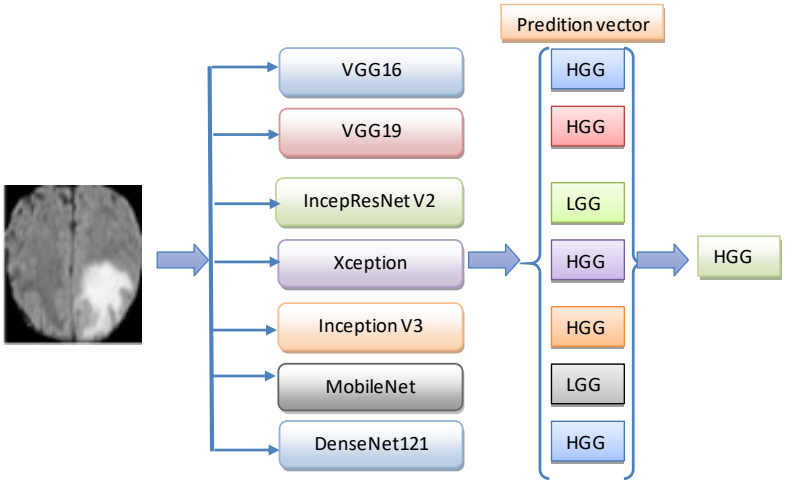

Figure 4. Stacking model using seven different pre-trained architecture and majority voting

2.5.1. VGG16 architecture

We use a VGG16 model with trainable and frozen layers as is shown in Figure 5.

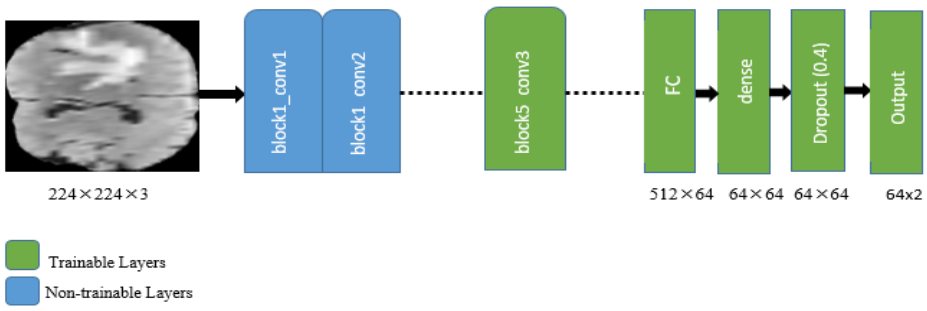

Figure 5. VGG16 Model with trainable and frozen layers

2.5.2. VGG19 architecture

The VGG-19 model is a trained convolutional neural network based on VGG-16 architecture. While the number 19 stands for the number of layers with trainable weights. In total, we have 16 convolutional layers and 3 fully connected layers. The distribution of the trainable layers and the fixed layers are shown in the Figure 6.

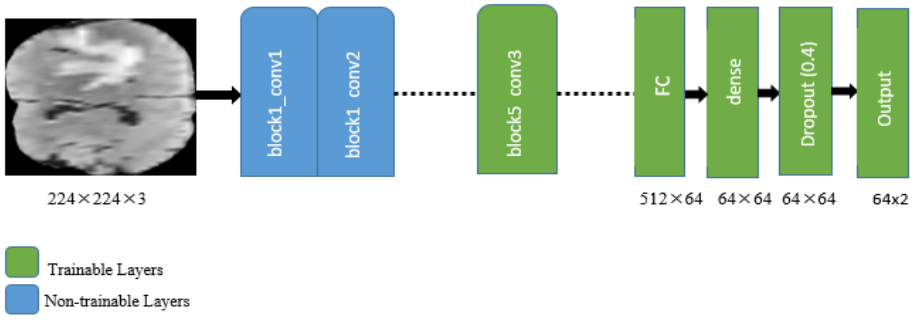

Figure 6. VGG-19 Model with trainable and frozen layers

2.5.3. MobileNet architecture

MobileNet architecture was proposed by Google. In our proposed model, the last four layers will be used for training our model based on our collected MR images while the rest of the layers are kept intact as is shown in Figure 7.

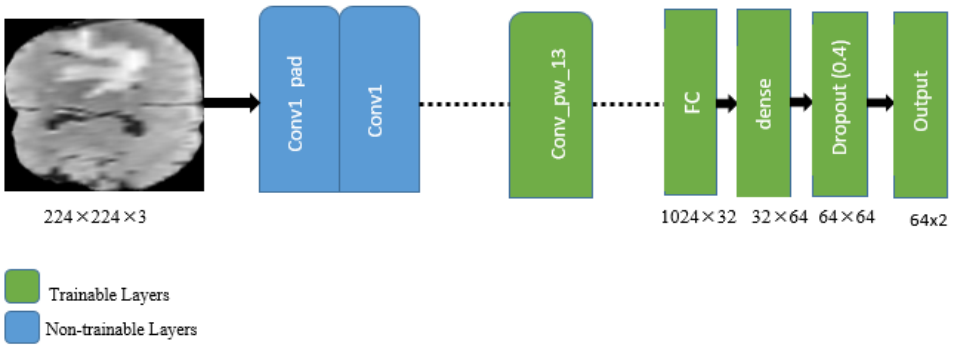

Figure 7. MobileNet model with trainable and frozen layers

2.5.4. InceptionV3 architecture

The inceptionV3 architecture is the third version introduced by Google to improve the Inception convolutional neural network and it is composed of 48 deep layers. In our proposed model, the layers from conv2d_92 to the last layer are kept intact while the rest of layers will be used for training our model based on our collected tumor MR images.

2.5.5. Xception architecture

Xception CNN model was developed by Francois Chollet. Its architecture is composed of 71 deep layers. In our proposed model, the last four layers will be used for training our model based on our collected tumor MR images while the rest of layers are kept intact.

2.5.6. InceptionResNetV2

In our proposed model, the last five layers will be used for training our model based on our collected tumor MR images while the rest of layers are kept intact as is shown in Figure 8.

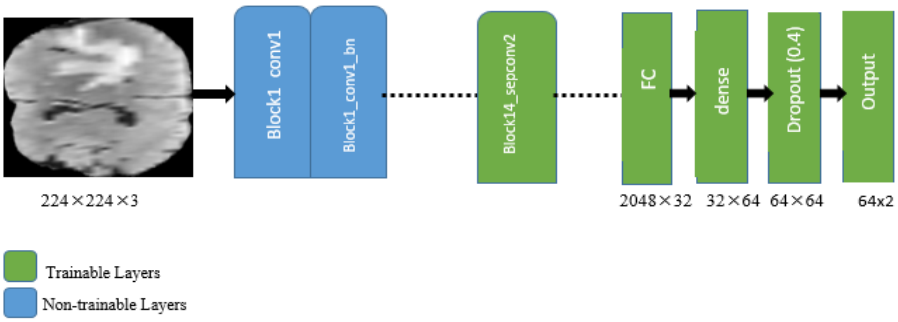

Figure 8. InceptionResNetV2 Model with trainable and frozen layers

2.5.7. DenseNet121 architecture

Finally, in DenseNet121 architecture, each layer has as input all the outputs of the layers that precede it, making the network architecture very dense, allowing deep supervision. In our proposed model, the layers from conv5_block16_1_bn to the last layer are kept intact while the rest of layers will be used for training our model based on our collected tumor MR images.

3. SIMULATION RESULTS

We use the Keras library of the platform Python and Tensorflow to develop our architectures of the CNN. In order to increase the robustness of our classification model, we will use the notion of 10-interval cross-validation. For this, we divided our training data into 10 equal intervals and at each iteration we chose nine intervals for training and the tenth interval that remains for validation. Thus, the performance values of our model are given in the form of an average of the values cancelled during the 10 iterations and a standard deviation. We also used the Adam algorithm to optimize our CNN architectures, and we have defined the loss function through the notion of cross-entropy.

To characterize the performances of our proposed model we calculated, during the training and validation processes, the precision and the loss for each fold-cross-validation and for each CNN. We thus obtained several simulation curves and only the curves of the InceptionV3 architecture are presented as an example in this paragraph. Throughout our training process, we first measured the precision of our training process for each CNN model for each fold cross validation at each period. The curves obtained with 10-fold cross-validation for InceptionV3 are shown in Figure 9. Secondly, we measured the loss of our training process for each CNN model forming our system for each fold cross validation at each epoch. The curves obtained with 10-fold cross-validation for inceptionV3 are shown in Figure 10. Then, to characterize the performances of our proposed model throughout our validation process, we first measured the precision for each CNN model forming our system for each fold cross validation at each epoch. The curves obtained with 10-fold cross-validation for InceptionV3 are shown in Figure 10. Secondly, we measured the precision and the loss of our validation process for each CNN model forming our system for each fold cross validation at each epoch. The curves obtained with 10-fold cross-validation for InceptionV3 are shown in Figure 11 and Figure 12 respectively. The final performance of the model was reported by averaging values obtained from each fold. For evaluating the testing process we plotted the true positive rate (TPR) against the false positive

rate (FPR) (ROC curve) for each CNN of our Deep transfer learning model. The curve obtained for Inception V3 is shown in Figure 13 and the curve obtained for our stacking model is shown in Figure 14.

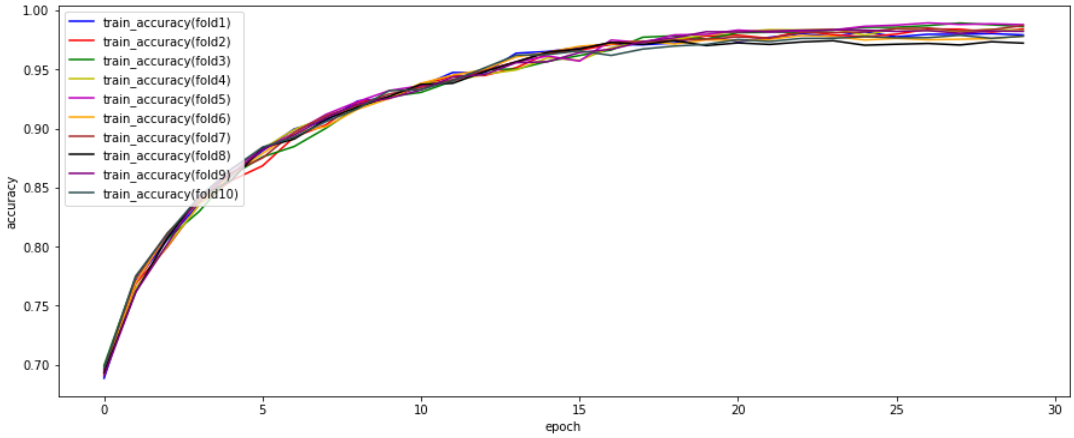

Figure 9. Train Accuracy versus epoch with 10-fold cross-validation for InceptionV3

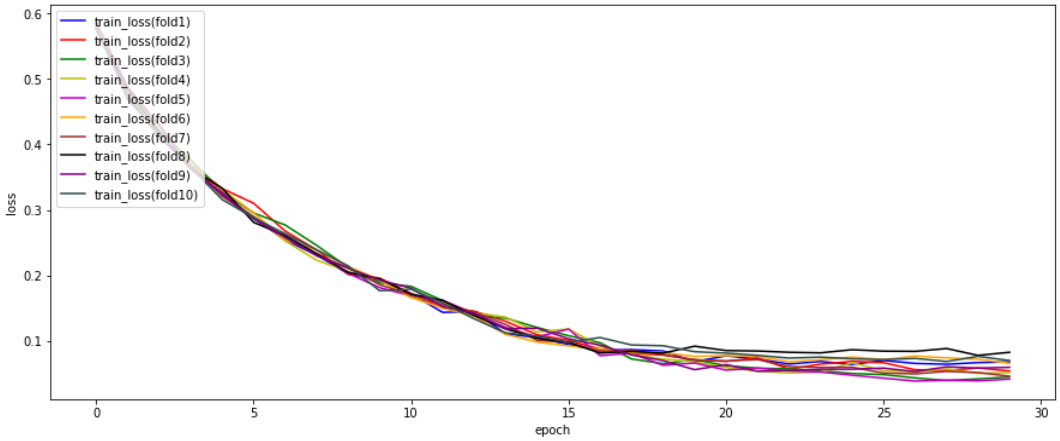

Figure 10. Train loss versus epoch with 10-fold cross- for InceptionV3

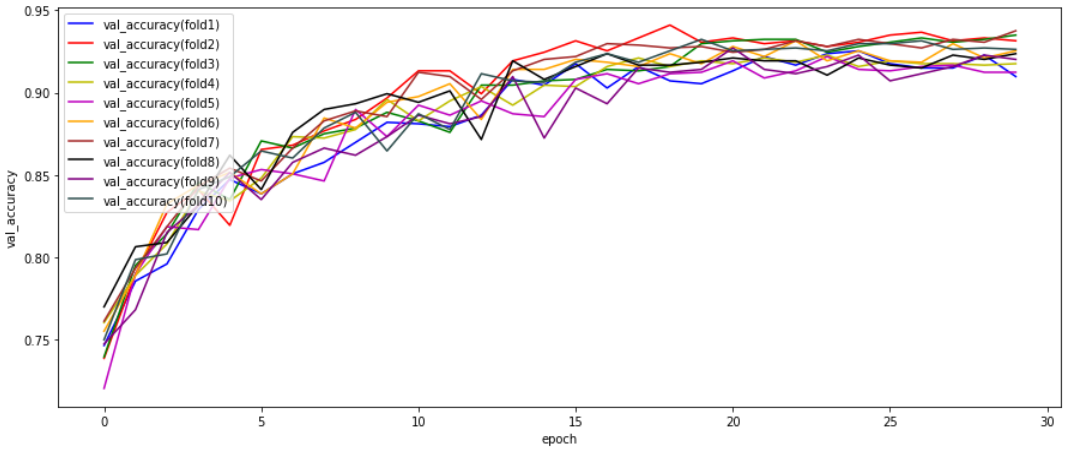

Figure 11. Validation Accuracy versus epoch with 10-fold cross-validation for InceptionV3

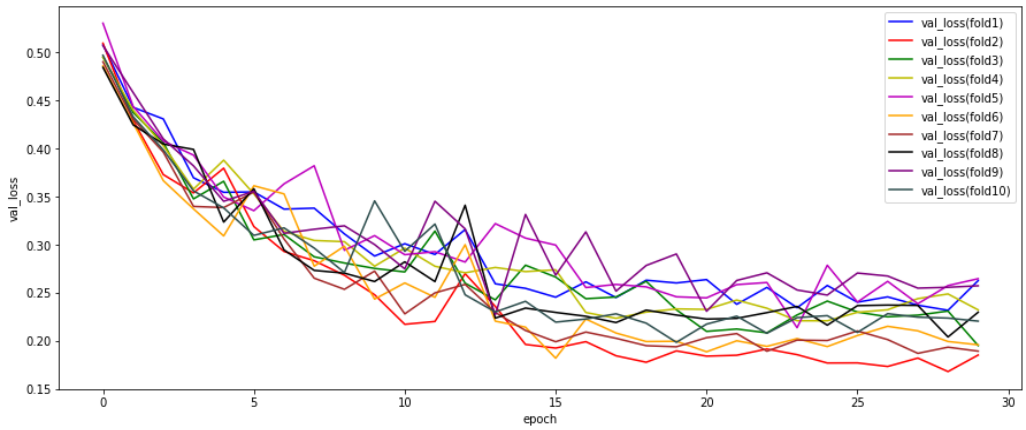

Figure 12. Validation loss versus epoch for with 10-fold cross-validation for InceptionV3

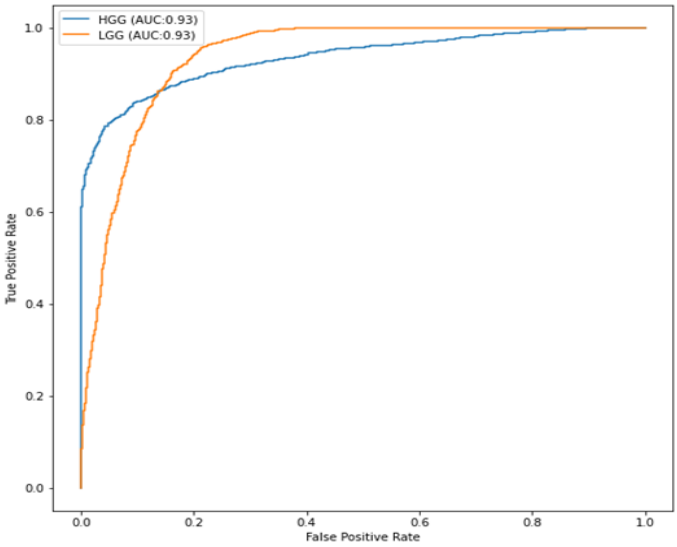

Figure 13. True positive rate (TPR) versus the false positive rate (FPR) (ROC curve) for InceptionV3 CNN

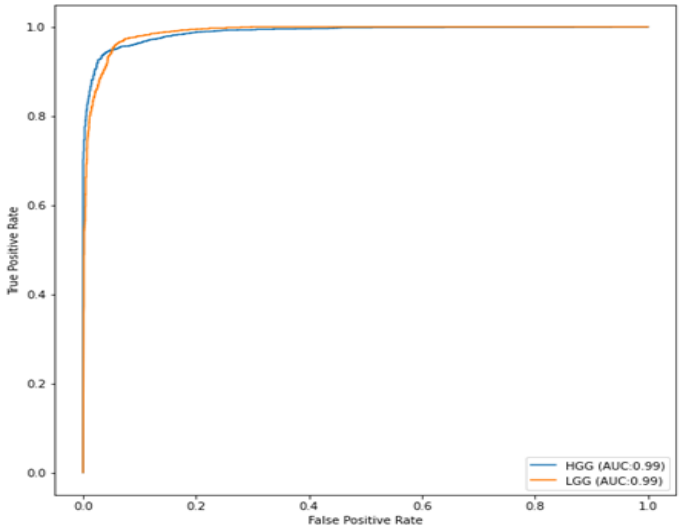

Figure 14. True positive rate (TPR) versus the false positive rate (FPR) (ROC curve) for our Stacking model

Performance of each class prediction results obtained by our proposed model during the validation of the training process is presented in Table 2. We found that the stacking model has allowed improving considerably the result obtained by each model taken individually. To evaluate the performance of our deep transfer learing model in its testing process, we calculated for each CNN network, the average value of the precision, sensitivity, F1 score and accuracy that we plotted on the Table 3. We have also reported on the last row of this table the performance measurements obtained by our stacking model. According to this table, the architectures which gave better precision are that of the VGG16 network and the InceptionResNetV2 network. In addition, the use of the stacking model has significantly improved the performance of our proposed global model, thus obtaining an accuracy of 98.67% and a sensitivity of 98.64% during the test process.

Table 2. The prediction results during the validation of the training process with 10-fold cross-validaion for each class using the model set which combines the seven models

Model	Average Precision (%) (±SD)		Average Sensitivity (%)(±SD)		Average F1-score (%)(±SD)	
	HGG	LGG	HGG	LGG	HGG	LGG
VGG16	99.35(±0.009)	96.21(±0.011)	96.31(±0.007)	99.57(±0.010)	97.21(±0.006)	97.01(±0.012)
VGG19	99.01(±0.007)	94.20(±0.009)	94.31(±0.005)	99.14(±0.008)	96.60(±0.004)	96.22(±0.010)
MobileNet	99.52(±0.011)	93.11(±0.013)	93.02(±0.009)	99.27(±0.012)	96.78(±0.009)	96.11(±0.014)
InceptionV3	97.40(±0.015)	92.09(±0.017)	92.51(±0.013)	97.23(±0.017)	94.07(±0.011)	94.02(±0.017)
Xception	95.47(±0.008)	89.31(±0.010)	88.03(±0.010)	95.24(±0.014)	92.28(±0.009)	92.23(±0.015)
InceptionResV2	93.42(±0.013)	97.20(±0.017)	97.10(±0.011)	93.31(±0.014)	95.26(±0.010)	95.22(±0.016)
DenseNet121	96.33(±0.017)	92.13(±0.019)	91.21(±0.015)	96.64(±0.018)	94.10(±0.014)	94.01(±0.019)
Proposed methode	99.99	97.29	97.62	99.99	98.59	99.01

Table 3. Comparative average results with standard deviation (SD) for each model on the test process.

Architecture	Average Precision (%) (SD)	Average Sensitivity (%) (SD)	Average F1-score (%) (SD)	Average Accuracy (%) (SD)
VGG16	94.56(±0.009)	95.87(±0.004)	95.21(±0.006)	95.16(±0.007)
VGG19	92.21(±0.017)	95.45(±0.015)	93.80(±0.014)	93.68(±0.014)
MobileNet	91.62(±0.015)	96.29(±0.008)	93.89(±0.011)	93.71(±0.012)
InceptionV3	90.49(±0.008)	93.71(±0.005)	92.07(±0.006)	91.78(±0.006)
Xception	89.78(±0.012)	91.26(±0.014)	90.50(±0.007)	90.39(±0.006)
InceptionResV2	94(±0.015)	94.41(±0.019)	95.48(±0.009)	95.45(±0.001)
DenseNet121	90.46(±0.008)	93.83(±0.007)	92.11(±0.006)	91.97(±0.007)
Proposed methode	98.67	98.64	98.62	98.06

4. COMPARISON STUDY

To compare our results with those published in the literature, we have gathered in Table 4 the results obtained by several researchers within the brain tumors classification framework. Afshar *et al*. [27], the authors evaluated their method and achieved an accuracy of 86.56%. Zia *et al*. [28], the authors could not exceed an accuracy of 85.69%. Cheng *et al* [29], the authors obtained an accuracy of 91.28%. Sajjad *et al*. [30], the authors significantly improved the value of their precision by obtaining an accuracy of 94.58%. Papageorgiou *et al*. [31], the authors could not exceed a precision of 92% by classifying the tumors in two classes: high degree and low degree. Barker *et al*. [32] the authors obtained a precision of 93.1%. Our proposed model reached an accuracy of 98.06% in the test prossus exceeding most of the obtained results in literature.

Table 4. Comparison with related works

Method	Sensitivity	Specificity	Accuracy
P. Afshar *et al*.[29]	-	-	86.56
R. Zia *et al.* [30]	86.26	90.90	85.69
J. Cheng *et al*. [31]	81	92	91.28
M. Sajjad [32]	88.41	96.12	94.58
Proposed method	98.64	98.67	98.06
E. Papageorgiou *et al.* [31]	-	-	92
J. Barker *et al.* [32]	-	-	93.1

5. DISCUSSION

In this article, we have proposed an intelligent clinical decision support system for the detection and classification of brain tumor from RMI images. We are interested in binary classification instead of multiclass classification because the proposed application will be used in rural and isolated areas by general practitioners who are not specialists in lung cancer. The goal of this work is that these doctors, thanks to this intelligent tool, can detect cancer early in order to be able to refer the patient to a specialized service for rapid and early treatment. To overcome the lack of databases to train the proposed CNN model, we have proposed a model that combines two notions: deep transfer learning and the stacking model. With deep transfer learning we have kept the cost of complex layer parameters and lengthy validation processes down. With the proposed stacking model, we have improved the performance of our model by best combining the predictions of several powerful machine learning models. For this, we used seven CNN architectures already pre-trained on an ImageNet dataset that we fitted precisely on a dataset of brain tumor images collected from the BraTS 2019 database. Furthermore we used 10-fold-cross-validation approach to evaluate the performance of our main 2-class model. With the proposed model we obtained an average test precision of 98.67%, an average f1 score of 98.62%, an average test precision of 98.06% and an average test sensitivity of 98.33%. With these results, it can be confirmed that the proposed model can be used to detect and classify brain tumors with precision and speed, especially since it succeeds in discriminating a low-grade tumor from a high-grade tumor.

6. CONCLUSION

In this article, we have proposed an intelligent clinical decision support system for the detection and classification of brain tumor from RMI images. To overcome the problem of the lack of labeled training data needed to train convolutional neural networks, we have proposed a model based on deep transfer learning and on the stacking models. With deep transfer learning we have eliminated the problems of the scarcity of queried data as well as the computational cost of complex layer parameters of long validation processes. With the stacking model we have improved the final precision of our model. For this, we used seven CNN architectures already pre-trained on an ImageNet dataset that we fitted precisely on a dataset of brain tumor images collected from the BraTS 2019 database. Weights of the layers of each network already pre-trained and we trained only the last layers of the network on our collected MRI image dataset. In this way, we ensured rapid and precise convergence of our model. In addition, to improve the accuracy of our global model, we will only predict as output the prediction that obtained the maximum score among the predictions of the seven pre-trained CNNs. We used a 10-way cross-validation approach to evaluate the performance of our main 2-class HGG and LGG model. The proposed model is more efficient with an average test precision of 98.67%, an average f1 score of 98.62%, an average test precision of 98.06% and an average test sensitivity of 98.33%. The results of our proposed approach exceed those obtained from other methods in literature.

REFERENCES

[1] H. Mohsen, E. S. A. El-Dahshan, E. S. M. El-Horbaty, and A. B. M. Salem, "Classification using deep learning neural networks for brain tumors," *Future Computing and Informatics Journal*, vol. 3, no. 1, pp. 68-71, 2018, doi: 10.1016/j.fcij.2017.12.001.

[2] A. Işın, C. Direkoğlu, and M. Şah, "Review of MRI-based brain tumor image segmentation using deep learning methods," *Procedia Computer Science*, vol. 102, pp. 317-324, 2016, doi: 10.1016/j.procs.2016.09.407.

[3] V. G. P. Rathi and S. Palani, "Brain tumor detection and classification using deep learning classifiers on MRI images," *Research Journal of Applied Sciences, Engineering, and Technology*, vol. 10, no. 2, pp. 177-187, 2015.

[4] Z. Sobhaninia, *et al*., "Brain tumor segmentation using deep learning by type-specific sorting of images," *arXiv preprint arXiv:1809.07786*, 2018.

[5] S. Deepak and P. M. Ameer, "Brain tumor classification using deep CNN features via transfer learning," *Computers in Biology and Medicine*, vol. 111, 2019, doi: 10.1016/j.compbiomed.2019.103345.

[6] E. Sert; F. Özyurt, and A. Do ˘gantekin, "A new approach for brain tumor diagnosis system: Single image super resolution based maximum fuzzy entropy segmentation and convolutional neural network," *Med. Hypotheses*, vol. 133, 2019, doi: 10.1016/j.mehy.2019.109413.

[7] Cancer.Net, Brain Tumor Statistics, 2021. Accessed: July, 2020. [Online]. Available: https://www.cancer.net/cancer-types/brain-tumor/statistics

[8] H. Dong, G. Yang, F. Liu, Y. Mao, and Y. Guo, "Automatic brain tumor detection and segmentation using unit-based fully convolutional networks," *Annual conference on medical image understanding and analysis*, 2017, pp. 506-517.

[9] M. Sajjad, S. Khan, K. Muhammad, W. Wu, A. Ullah, and S.W. Baik," Multi-grade brain tumor classification using deep CNN with extensive data augmentation," *Journal of Computational Science*, vol. 30, pp. 174-182, 2019, doi: 10.1016/j.jocs.2018.12.003.

[10] P. Korfiatis, T. L. Kline and B. J. Erickson, "Automated segmentation of hyperintense regions in FLAIR MRI using deep learning," *Tomography*, vol. 2, no. 4, pp. 334-340, 2016, doi: 10.18383/j.tom.2016.00166.
[11] S. Roy and S. K. Bandyopadhyay, "Detection and Quantification of Brain Tumor from MRI of Brain and It's Symmetric Analysis," *Int. J. Inf. Commun. Technol. Res*., vol. 2, no. 6, pp. 477–483, 2012.
[12] S. Pereira, A. Pinto, V. Alves, and C. A. Silva, "Brain Tumor Segmentation Using Convolutional Neural Networks in MRI Images," *IEEE Transactions on Medical Imaging*, vol. 35, no. 5, pp. 1240-1251, May 2016, doi: 10.1109/TMI.2016.2538465.
[13] A. Tiwari, S. Srivastava, and M. Pant, ,"Brain tumor segmentation and classification from magnetic resonance images: Review of selected methods from 2014 to 2019," *Pattern Recognition Letters*, vol. 131, pp. 244–260, 2020, doi: 10.1016/j.patrec.2019.11.020.
[14] U. N. Hussain, *et al*., "A Unified Design of ACO and Skewness based Brain Tumor Segmentation and Classification from MRI Scans," *J. Control Eng. Appl. Inf.*, vol. 22, no. 2, pp. 43–55, 2020.
[15] Z. N. K. Swati, *et al*., "Brain tumor classification for MR images using transfer learning and fine-tuning," *Computerized Med. Imaging and Graphics*, vol. 75, pp. 34–46, 2019, doi: 10.1016/j.compmedimag.2019.05.001.
[16] A. Gumaei, M. M. Hassan, M. R. Hassan, A. Alelaiwi, and G. Fortino, "A Hybrid Feature Extraction Method with Regularized Extreme Learning Machine for Brain Tumor Classification," *IEEE Access*, vol. 7, pp. 36266-36273, 2019, doi: 10.1109/ACCESS.2019.2904145.
[17] A. Mesbah, A. Berrahou, H. Hammouchi, H. Berbia, H. Qjidaa, and M. Daoudi, "Lip reading with Hahn Convolutional Neural Networks," *Img. and Vis. Comp.*, vol. 88, pp. 76-83, 2019, doi: 10.1016/j.imavis.2019.04.010.
[18] C. Zhou, S. Chen, C. Ding, and D. Tao, "Learning contextual and attentive information for brain tumor segmentation," *Int. MICCAI Brainlesion Workshop*, 2018, pp. 497-507, doi: 10.1007/978-3-030-11726-9_44.
[19] T. E. Liang, U. U. Sheikh, and M. N. H. Mohd, "Malaysian car plate localization using region based convolutional neural network," *Bulletin of Electrical Engineering and Informatics*, vol. 9, no. 1, pp.411-419, 2020, doi: 10.11591/eei.v9i1.1862.
[20] B. H. Menze, *et al*., "The Multimodal Brain Tumor Image Segmentation Benchmark (BRATS)," *IEEE Transactions on Medical Imaging*, vol. 34, no. 10, pp. 1993-2024, Oct. 2015, doi: 10.1109/TMI.2014.2377694.
[21] T. H. Phan, D. C. Tran, and M. F. Hassan, "Vietnamese character recognition based on CNN model with reduced character classes," *Bulletin of Electrical Engineering and Informatics*, vol. 10, no.2, pp. 962-969, 2020, doi: 10.11591/eei.v10i2.2810.
[22] Y. Bhatia, A. Bajpayee, D. Raghuvanshi, and H. Mittal, "Image Captioning using Google's Inception-resnet-v2 and Recurrent Neural Network," *2019 Twelfth International Conference on Contemporary Computing (IC3)*, 2019, pp. 1-6, doi: 10.1109/IC3.2019.8844921.
[23] G. Huang, Z. Liu, L. Van Der Maaten, and K. Q. Weinberger, "Densely Connected Convolutional Networks," *2017 IEEE Conference on Computer Vision and Pattern Recognition (CVPR)*, 2017, pp. 2261-2269, doi: 10.1109/CVPR.2017.243.
[24] N. R. Gavai, Y. A. Jakhade, S. A. Tribhuvan, and R. Bhattad, "MobileNets for flower classification using TensorFlow," *2017 International Conference on Big Data, IoT and Data Science (BID)*, 2017, pp. 154-158, doi: 10.1109/BID.2017.8336590.
[25] C. Szegedy, S. Ioffe, V. Vanhoucke, and A. A. Alemi, "Inception-v4, fInception-ResNet and the Impact of Residual Connections on Learning," *Proceedings of the Thirty-First AAAI Conference on Artificial Intelligence*, 2017, pp. 4278-4284.
[26] F. Chollet, "Xception: Deep Learning with Depthwise Separable Convolutions," *2017 IEEE Conference on Computer Vision and Pattern Recognition (CVPR)*, 2017, pp. 1800-1807, doi: 10.1109/CVPR.2017.195.
[27] P. Afshar, A. Mohammadi, and K. N. Plataniotis, "Brain Tumor Type Classification via Capsule Networks," *2018 25th IEEE International Conference on Image Processing (ICIP)*, 2018, pp. 3129-3133, doi: 10.1109/ICIP.2018.8451379.
[28] R. Zia, P. Akhtar, and A. Aziz, "A new rectangular window based image cropping method for generalization of brain neoplasm classification systems," *International Journal of Imaging Systems and Technology*, vol. 28, no. 3, pp. 153-162, 2018, doi: 10.1002/ima.22266.
[29] J. Cheng, *et al*., "Enhanced performance of brain tumor classification via tumor region augmentation and partition," *PloS one*, vol. 10, no. 12, p. e0140381, 2015, doi: 10.1371/journal.pone.0140381.
[30] M. Sajjad, S. Khan, K. Muhammad, W. Wu, A. Ullah, and S. W. Baik, "Multi-Grade Brain Tumor Classification using Deep CNN with Extensive Data Augmentation," *Journal of Computational Science*, vol. 30, pp. 174-182, 2018, doi: 10.1016/j.jocs.2018.12.003.
[31] E. I. Papageorgiou, *et al*., "Brain tumor characterization using the soft computing technique of fuzzy cognitive maps," *Applied Soft Computing*, vol. 8, pp. 820-828, 2008, doi: 10.1016/j.asoc.2007.06.006.
[32] J. Barker, A. Hoogi, A. Depeursinge, and D. L. Rubin, "Automated classification of brain tumor type in whole-slide digital pathology images using local representative tiles," *Medical Image Analysis*, vol. 30, pp. 60-71, 2016, doi: 10.1016/j.media.2015.12.002.